



Sound attenuation using duct silencers with micro-perforated panel absorbers

Xiang YU¹; Li CHENG¹; Yuhui Tong²; Jie PAN²

¹The Hong Kong Polytechnic University, Hong Kong

²The University of Western Australia, Australia

ABSTRACT

Micro-perforated panel (MPP) can be used as non-fibrous acoustic absorber which can provide broadband sound absorption performance. In this study, a sub-structuring methodology based on the Patch Transfer Function (PTF) approach to deal with duct silencers with MPP absorbers and internal partitions is proposed, and the sound attenuation performance of such silencers is investigated. Reactive silencers with only internal partitions are shown to exhibit strong resonant pattern, with each sub-divided chamber acting as acoustic resonators for strong sound reflection. On the other hand, hybrid silencers which combine the reactive effect of partitions and dissipative effect of MPP absorbers are studied. Simulation results show that MPP parameters such as hole diameters have strong influence on the silencing performance. Although the hole diameter of MPP is typically very small (less than 1mm), the reactive effect of MPP silencer is still obvious. The calculation accuracy of the proposed formulation is validated against finite element method (FEM) analysis.

Keywords: Silencer, Micro-perforated panel I-INCE Classification of Subjects Number(s): 31.4, 35.6

1. INTRODUCTION

In recent years, MPP absorbers as promising alternatives to conventional sound absorbing materials have attracted many researcher's attentions. MPP typically consists of a thin metal sheet with distributed perforation holes in sub-millimeter size. The acoustic impedance model developed by Maa (1) regards the small perforation holes as a lattice of short narrow tubes, with an end correction term being added to account for the attached air mass on both ends. To form a basic MPP absorber, a backing cavity is generally required, and the dependence of its absorption performance on various driving parameters has been discussed (1).

Due to its excellent material properties such as non-fibrous, incombustible, and cleanable, MPP absorbers have found their uses in a wide range of practical applications. For example, Asdrubali and Pispola (2) constructed noise barriers based on transparent polycarbonate MPPs, which exhibit good acoustical and optical performances. Park (3) investigated the acoustic behavior of MPP absorber backed by Helmholtz resonator for low-frequency performance improvement, and examined its applicability in reducing the noise level inside a launcher fairing. Herrin et al. (4) attempted to enhance the MPP absorption in a rectangular enclosure by partitioning the backing cavity with honeycomb structure, aiming at applications for construction equipments, buildings, and acoustic silencers.

About fifteen years ago, a preliminary study on using MPP absorbers for noise control inside a duct was performed by Wu (5), where the MPP surface is considered as a locally reacting boundary. As such, MPP together with the backing cavity system is equivalent to an absorptive surface, whose acoustic impedance can be calculated using the formula given in reference (1). However, due to the limitation of that assumption, the predicted results were not accurate enough compared with experiments. More recently, Allam and Abom (6) proposed a new type of dissipative silencer based on MPPs, which can deliver comparable silencing performance to a dissipative silencer filled with porous materials. However, it is noted that apart from these studies, investigations on the acoustic behavior of MPPs in silencer applications are still lacking in the open literature.

¹ 11901366r@connect.polyu.hk

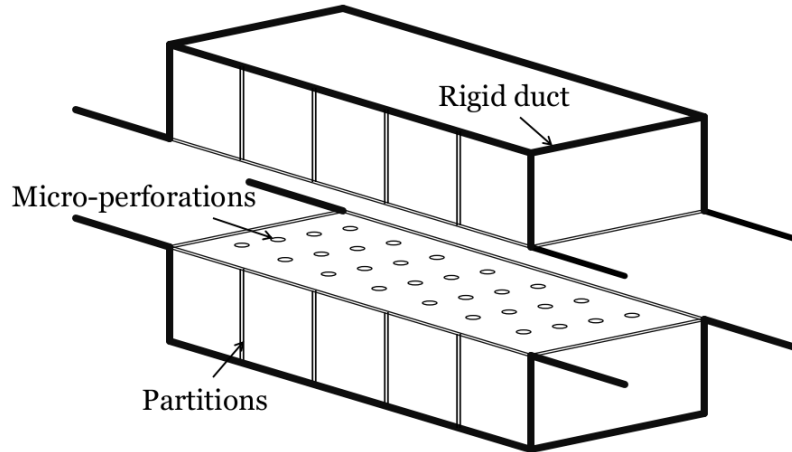


Figure 1 - An example of duct silencer with MPP for sound absorption.

Figure 1 presents a typical MPP silencer with expansion volume covered with sound absorbing panels. The solid partitions inside the backing cavity are to enhance the locally reactive behavior of MPP (4) and at the same time, provide some reinforcement for the thin MPP surface. In order to deal with such system, this paper proposes a three-dimensional sub-structuring approach based on the Patch Transfer Function (PTF) method (7,8), to deal with the existence of MPPs and internal partitions. The side-branch configuration is modeled as a combination of multiple unit cells, with each cell comprising a MPP facing and a backing acoustic cavity. The major objectives of the present study are to capture the hybrid noise attenuation mechanism, to analyze the possible influence of system parameters, and to provide a versatile simulation tool for possible system optimization in the future.

Following this introduction, the proposed PTF formulation together with the unit cell treatment is presented. Reactive silencers with only internal partitions are first discussed to serve as benchmarks, which exhibit narrow band TL characteristics due to the resonator effect. The acoustic behavior after adding MPP to the reactive chamber is then investigated, and the hybrid effect of sound reflection and absorption is analyzed. The study on the MPP parameter shows that there exists considerable room for possible performance tuning. The accuracy and convergence of the calculations are validated through comparisons with FEM analysis.

2. FORMULATION

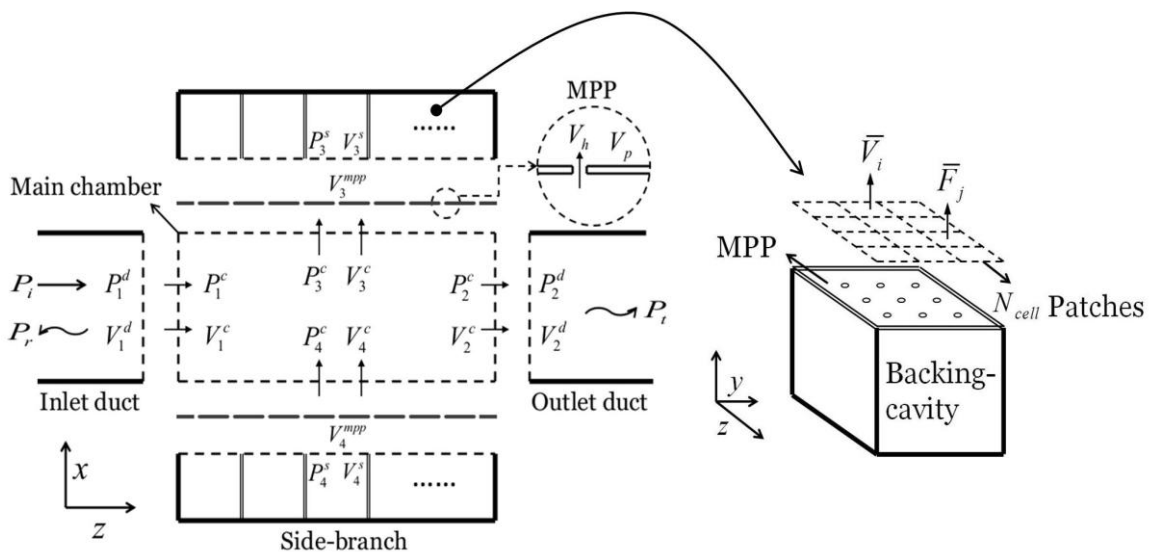


Figure 2 - Sub-structuring framework for a MPP silencer and unit cell treatment for the side-branch cavity.

Consider the MPP silencer as shown in figure 1, the solid partitions behind MPP divide the side-branch cavity into multiple chamber units. The sub-structuring treatment of the global system is illustrated in figure 2, where the silencer domain is decoupled into inlet/outlet ducts, main chamber, and two side-branches. The main chamber is connected with the surrounding acoustic domains through the four coupling interfaces numbered from 1 to 4.

In several earlier publications (references 7-9), the basic steps of using the PTF approach have been well-established, and will not be repeated here due to the page limitation. The PTF coupling framework for the present MPP silencer is similar to that of a reactive silencer as presented in reference (8), and the subsystem patch transfer functions (PTFs) to be determined are summarized as follows: duct radiation impedances Z^d at interfaces 1 and 2; 16 surface-to-surface impedances Z^c for the main chamber; side-branch cavity impedances Z^{sc} and surface mobilities Y^{sc} at interfaces 3 and 4, respectively. Note that all these quantities are calculated before the assembly to form a set of database. Then, according to the normal direction notations in figure 2, the systematic equations to describe the fully coupled system in the linear regime are established as (8):

$$\begin{aligned}
 \tilde{F} + Z_1^d V_1^d &= Z_{11}^c V_1^c + Z_{12}^c V_2^c + Z_{13}^c V_3^c + Z_{14}^c V_4^c \\
 Z_{21}^c V_1^c + Z_{22}^c V_2^c + Z_{23}^c V_3^c + Z_{24}^c V_4^c &= Z_2^d V_2^d \\
 Y_3^{sc} (Z_{31}^c V_1^c + Z_{32}^c V_2^c + Z_{33}^c V_3^c + Z_3^{sc} V_3^{sc} + Z_{34}^c V_4^c) &= V_3^{sc} \\
 Y_4^{sc} (Z_{41}^c V_1^c + Z_{42}^c V_2^c + Z_{43}^c V_3^c + Z_{44}^c V_4^c + Z_4^{sc} V_4^{sc}) &= V_4^{sc}
 \end{aligned} \tag{1}$$

where patch forces at interfaces 1 and 2 between the main chamber and inlet/outlet ducts are required to be continuous; the coupling between the main chamber and side-branch cavities is formulated by treating MPP as a structural interface.

The PTF calculations of conventional subsystems, including duct and main chamber impedance, have been detailed in reference (9). Here, the remaining challenge comes from the modeling of the side-branch cavity. In figure 2, the side-branch cavity can be viewed as a series of unit cells, with each cell comprising a MPP facing and a backing rectangular cavity. Note that the parameters of each unit cell can be different.

The side-branch impedance Z^{sc} and mobility Y^{sc} are obtained by combining all the unit cells to form an elements array. For the modeling of the MPP in a unit cell, the hole impedance formula by considering the perforated holes as a lattice of short narrow tubes gives (1)

$$Z_h = \frac{32\eta t}{d^2} \left[\left(1 + \frac{k^2}{32}\right)^{1/2} + \frac{\sqrt{2}}{32} k \frac{d}{t} \right] + j\rho_0 \omega t \left[1 + \left(1 + \frac{k^2}{32}\right)^{-1/2} + 0.85 \frac{d}{t} \right] \tag{2}$$

where ρ_0 is the air density, η is the air viscosity, t and d are the thickness and hole diameter of MPP, $k = d\sqrt{\rho_0\omega/4\eta}$. The term $0.85d/t$ is used to characterize the end correction effect.

If the panel frame of MPP is rigid, the averaged air velocity in the vicinity of MPP surface V_{mpp} can be obtained by averaging the vibrational velocity inside the perforated holes with the rigid panel frame:

$$V_{mpp} = \sigma V_h \tag{3}$$

where V_h is the air velocity inside the holes, σ is the perforation ratio.

When a pressure difference is subjected to both sides of MPP surface, the hole mass velocity is expressed as:

$$\Delta p = Z_h V_h \quad (4)$$

Since the distance between perforated holes is much larger than their diameters and the panel frame is not vibrating, the cross-coupling between patches among a MPP surface is generally weak. Thus, the MPP mobility of a unit cell is a diagonal matrix, with corresponding diagonal terms equal to

$$Y_{mpp} = \frac{V_{mpp}}{\Delta p \times S} = \frac{\sigma}{Z_h S} \quad (5)$$

where S is the surface area of the segmented patch.

As to the modeling of the backing-cavity behind MPP, the present formulation considers it as a three-dimensional rectangular cavity. Based on the modal expansion theory, the backing-cavity impedance of a unit cell is obtained as (9):

$$Z^c = \frac{\bar{F}_i^c}{\bar{V}_j^c} = \sum_r \frac{j\rho_0\omega}{N_c^r(k^2 - k_r^2)} \int_{S_i} \varphi_c^r dS_i \int_{S_j} \varphi_c^r dS_j \quad (6)$$

Since the unit cells are well separated from each other by the rigid partitions, the cross-coupling between them is deemed as weak. Therefore, the side-branch mobility Y^{sc} and impedance Z^{sc} at interfaces 3 and 4 can be constructed by combining all the unit cells in a common subsystem:

$$Y^{sc} = \begin{bmatrix} Y_{mpp}^I & & & \\ & Y_{mpp}^{II} & & \\ & & Y_{mpp}^{III} & \\ & & & \ddots \end{bmatrix}; \quad Z^{sc} = \begin{bmatrix} Z_c^I & & & \\ & Z_c^{II} & & \\ & & Z_c^{III} & \\ & & & \ddots \end{bmatrix} \quad (7)$$

In addition to Eq. (1), the system response at each coupling interface is obtained by applying the velocity continuity condition at the connecting patches:

$$\begin{aligned} V_1^d &= V_1^c, V_2^c = V_2^d; \quad \text{at interfaces 1, 2} \\ V_3^c &= V_3^{sc}, V_4^c = V_4^{sc}; \quad \text{at interfaces 3, 4} \end{aligned} \quad (8)$$

As shown in figure 2, the sound pressure field inside the inlet duct is a combination of incident and reflected sound waves, and that inside the outlet duct is the transmitted sound waves. Once the patch velocity response has been solved, the silencing performance can be evaluated by calculating the sound transmission loss,

$$TL = 10 \log_{10} \left(\frac{1}{\tau} \right) \quad (9)$$

where τ is the ratio between the transmitted and incident sound power $\tau = \Pi_2^t / \Pi_1^i$.

The incident sound power Π_1^i at interface 1 corresponding to a normal plane wave incidence with pressure amplitude equals to p_0 is

$$\Pi_1^i = \frac{|p_0|^2}{2\rho_0 c_0} S_1 \quad (10)$$

where S_1 is the total surface area of the incident surface. As to the transmitted sound power

due to patch vibration at interface 2,

$$\Pi_2^t = \frac{1}{2} \int_{S_2} \text{Re}\{P_2 \times V_2^*\} dS_2 \quad (11)$$

where P_2 is the radiated sound pressure into the outlet duct, calculated via duct radiation impedance Z^d as $P_2 = Z^d V_2$; S_2 is the area of the radiation surface; the asterisk for the patch velocity denotes its complex conjugate.

In order to reveal the hybrid attenuation mechanism of MPP silencer, the reactive effect and dissipative effect need to be separated. The reflection and absorption coefficients are used to quantify these effects. The reflection coefficient R is defined as the reflected sound power over the incident power at interface 1,

$$R = \frac{\Pi_1^r}{\Pi_1^i} = \frac{(\Pi_1^i - \Pi_1^t)}{\Pi_1^i} \quad (12)$$

where the reflected sound power Π_1^r is calculated by subtracting the incident power Π_1^i and transmitted power Π_1^t to the downstream, at interface 1:

$$\Pi_1^r = \frac{1}{2} \int_{S_1} \text{Re}\{P_1 \times V_1^*\} dS_1 \quad (13)$$

Similarly, the absorption coefficient α is defined as the percentage of sound power being absorbed by the silencer, which writes:

$$\alpha = \frac{(\Pi_1^i - \Pi_2^t)}{\Pi_1^i} \quad (14)$$

It is clear that the present 3-D modeling does not suffer from the plane wave assumption, which is an inherent limitation in the previous analyses on MPP silencers (5,6). Meanwhile, the proposed concept of unit cells provides a flexible tool to handle complex side-branch configurations, which could eventually allow a free-tuning of silencing performance in the later design stage.

3. SIMULATION RESULTS AND DISCUSSIONS

3.1 Reactive silencers for validation

The proposed sub-structuring formulation is employed to investigate the acoustic behavior of several typical silencer configurations based on figure 1. The basic silencer configuration is a rigid expansion chamber with a dimension of $0.3\text{m}(x) \times 0.1\text{m}(y) \times 0.5\text{m}(z)$, and the cross-section of the inlet/outlet duct is $0.1\text{m}(x) \times 0.1\text{m}(y)$. The whole system is excited by a plane wave with unity pressure amplitude at the inlet.

Before considering the effect of MPP, reactive silencers with only internal partitions are first studied to serve as benchmarks. In figure 3, the chamber length, being kept as 0.5m, is evenly divided into several sub-chambers by certain pairs of solid partitions, while the central airway is left open for the purpose of air passage. Figure 3 compares the predicted TLs using the present PTF approach with those obtained from FEM analyses using commercial software COMSOL. For the three silencer cases with single, dual, and five chambers, excellent agreements are observed between PTF calculations and FEM results, which validate the proposed formulation. The attenuation performance of the simplest empty chamber is generally weak along the frequency range. For the five-chamber silencer, the predicted TL shows a narrow sharp peak near 930Hz, while the TL performances at other frequencies are compromised. This sharp TL peak is actually due to the accumulative effect of connecting multiple identical unit cells in series, forming a kind of resonators array. The resonant frequency of each resonator cell is located at 930Hz.

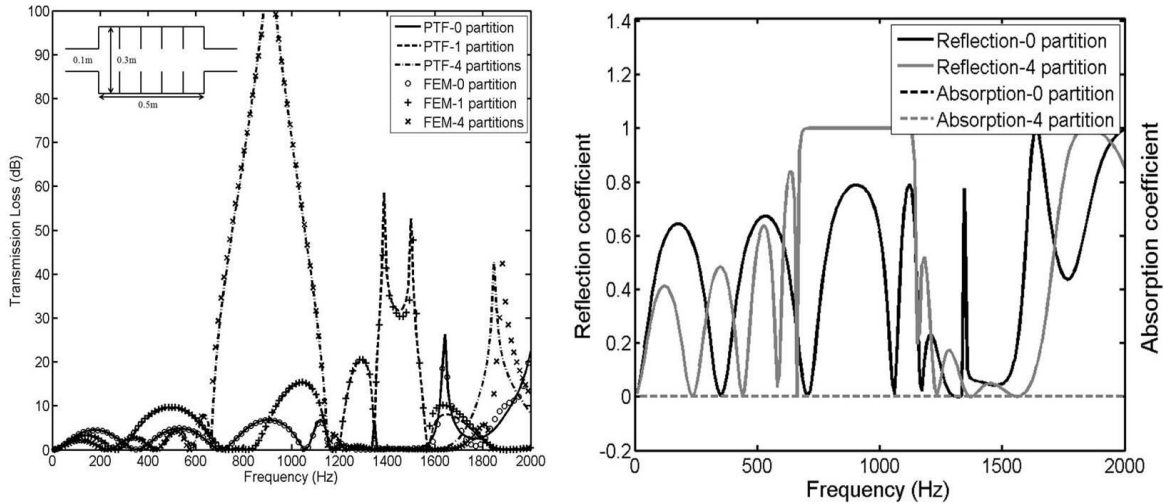


Figure 3 - Predicted TLs for reactive silencers and the reflection/absorption coefficients

As shown in figure 3, the reflection and absorption coefficients being defined in equations (12) and (14) are used to quantify the reactive effect and dissipative effect. For the two test cases, the trends of reflection coefficients ranging from zero to one exactly coincide with the TL curves, while the absorption coefficients are constantly zero. This means that the attenuation mechanism of such silencer purely depends on sound reflection.

3.2 Hybrid MPP silencers

When the MPP absorbers are added inside the chamber to cover the side-branch cavity, the predicted TLs using the proposed formulation is illustrated in figure 4, which also shows the effect of different MPP hole diameters on the silencing performance. It can be seen that with decreasing hole diameter from 1mm to 0.2mm, the TL bandwidth is generally widened, leading to an improved broadband attenuation behavior. The reason is that smaller hole diameter induces higher acoustic resistance, which is most effective in widening the absorption bandwidth.

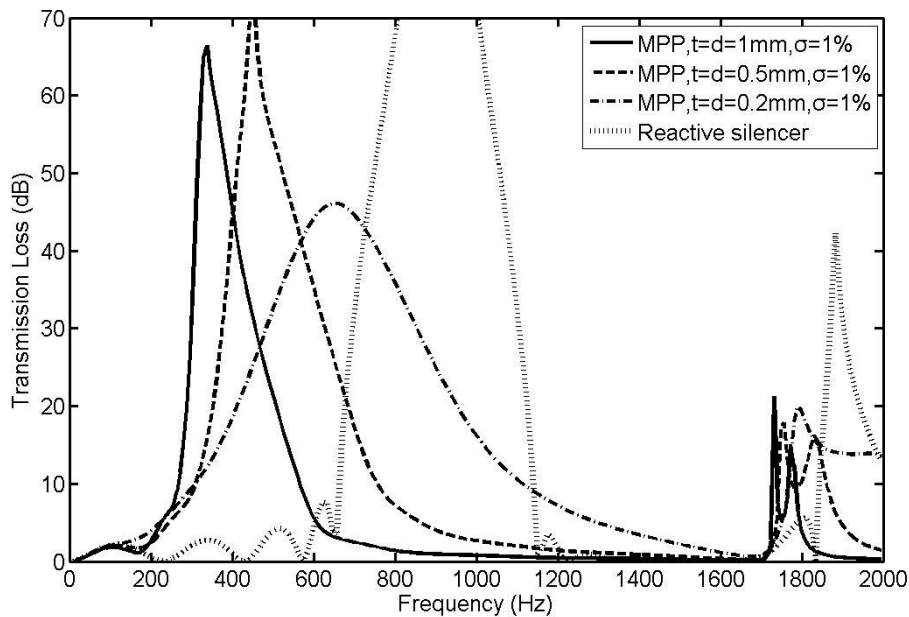


Figure 4 - Predicted TLs for MPP silencers with different hole diameters

On another aspect, the hybrid noise attenuation mechanism of such silencer is captured by separating the sound energy being reflected and absorbed. The reflection and absorption coefficients corresponding to the three MPP cases are calculated. In figure 5(a), it can be seen that although the MPP hole diameter is typically very small (less than 1mm), the reactive effect of such silencer still exists, which is more obvious with larger holes. The absorption coefficient in figure 5(b) shows that MPP with smaller holes can provide a broader absorptive performance, which is consistent with the TL comparison in figure 4. At the TL peaks, the dissipative effect is weakened, while the reactive effect is stronger to compensate the noise attenuation. Therefore, the attenuation mechanism of such silencer is actually a combination of reactive effect due to solid partitions and dissipative effect due to MPPs. This indicates that by carefully tuning and balancing the reactive and dissipative effects, the performance of such silencer can be further improved.

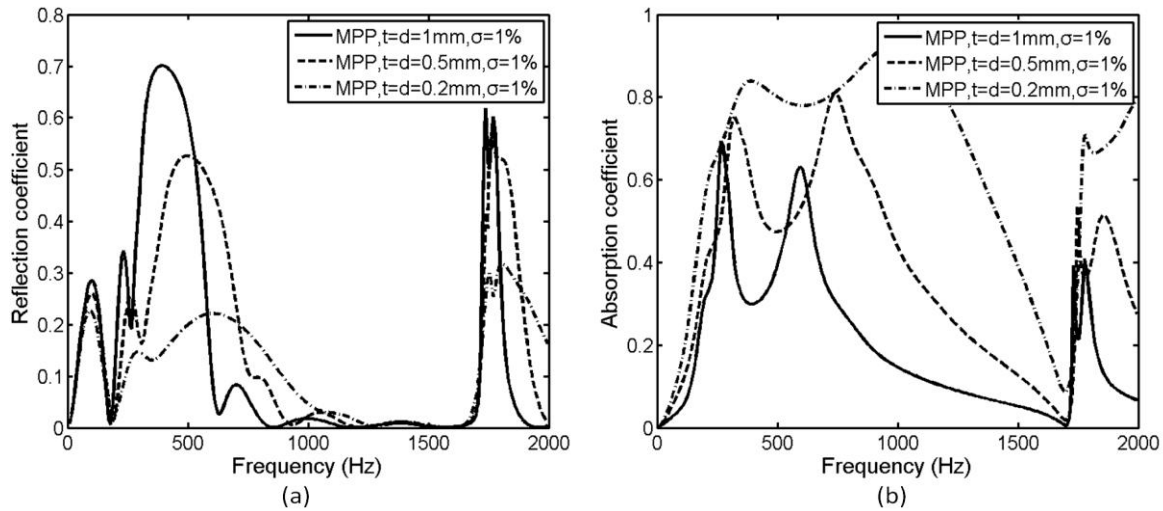


Figure 5 - Calculated reflection and absorption coefficients for MPP silencers

4. CONCLUSIONS AND REMARKS

A 3-D sub-structuring approach to model expansion chamber silencers with internal partitions and MPPs is proposed. The side-branch configuration is treated as a combination of unit cells connected in series, with each cell comprising a MPP facing and a backing cavity. The proposed formulation is employed to study various silencer configurations, which demonstrates its capability and flexibility in handling such systems. The effect of varying MPP parameters is shown, and the hybrid noise attenuation mechanism of MPP silencers is studied by separating the reactive and dissipative effects.

Although the present study focuses on relatively simple silencer geometries, the revealed physical phenomena can provide solid foundations for the better design of more practical silencers, for example, a heavy-truck silencer as shown in figure 6. The original poor silencing performance for the frequencies below 200Hz and beyond 350Hz can be possibly improved by adding internal resonators or MPP absorbers, by considering the physical understandings obtained from the present study. This could possibly serve as one direction for future studies.

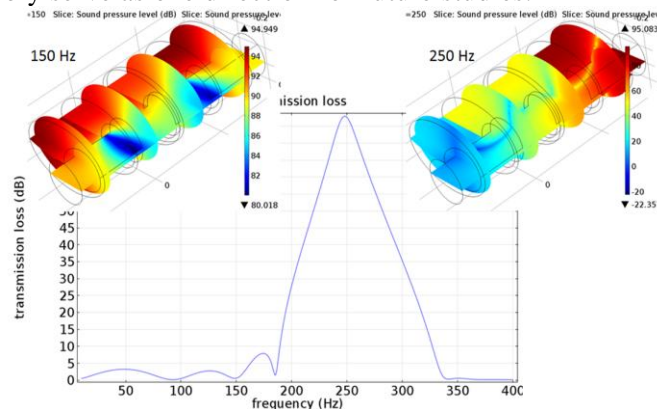


Figure 6 - A commercial heavy-truck silencer and its narrow TL behavior, tested at UWA.

ACKNOWLEDGEMENTS

The authors wish to acknowledge two grants from Research Grants Council of Hong Kong Special Administrative Region, China (PolyU 5103/13E and 152026/14E). The first author is grateful to the Research Office of HK PolyU for providing financial support for his exchange program at UWA.

REFERENCES

1. D. Y. Maa, "Potential of microperforated panel absorber," *J. Acoust. Soc. Am.* 104, 2861-2866 (1998)
2. F. Asdrubali and G. Pispola, "Properties of transparent sound-absorbing panels for use in noise barriers," *J. Acoust. Soc. Am.* 121, 214-221 (2007)
3. S. H. Park, "Acoustic properties of micro-perforated panel absorbers backed by Helmholtz resonators for the improvement of low-frequency sound absorption," *J. Sound Vib.* 332 4895-4911 (2013)
4. J. Liu and D. W. Herrin, "Enhancing micro-perforated panel attenuation by partitioning the adjoining cavity," *Appl. Acoust.* 71 120-127 (2010)
5. M. Q. Wu, "Micro-perforated panels for duct silencing," *Noise Control Eng.* 45, 69-77 (1997)
6. S. Allam and M. Åbom, "A new type of muffler based on microperforated tubes," *J. Vib. Acoust.* 133, 031005 (2011)
7. J. D. Chazot and J. L. Guyader, "Prediction of transmission loss of double panels with a patch-mobility method," *J. Acoust. Soc. Am.* 121, 267-278 (2007)
8. X. Yu, L. Cheng and J. L. Guyader, "Vibroacoustic modeling of cascade panels system involving apertures and micro-perforated elements," Conference paper, 20th International Congress on Sound & Vibration (2013)
9. X. Yu, L. Cheng and J. L. Guyader, "Modeling vibroacoustic systems involving cascade open cavities and micro-perforated panels," *J. Acoust. Soc. Am.* (In Press) (2014)
10. X. Yu, L. Cheng and J.L. Guyader, "On the modeling of sound transmission through a mixed separation of flexible structure with an aperture," *J. Acoust. Soc. Am.* 135, 2785-2796 (2014)